Article

An Improved Continuous Flow Analysis System for High-Resolution Field Measurements on Ice Cores

Patrik R. Kaufmann, Urs Federer, Manuel A. Hutterli, Matthias Bigler, Simon Schu#pbach, Urs Ruth, Jochen Schmitt, and Thomas F. Stocker

Environ. Sci. Technol., **2008**, 42 (21), 8044-8050 • DOI: 10.1021/es8007722 • Publication Date (Web): 04 October 2008

Environ. Sci. Technol. **2008,** *42,* 8044–8050

An Improved Continuous Flow Analysis System for High-Resolution Field Measurements on Ice Cores

PATRIK R. KAUFMANN,*,†,‡ URS FEDERER,†,‡ MANUEL A. HUTTERLI,§ MATTHIAS BIGLER,∥ SIMON SCHÜPBACH,†,‡ URS RUTH,⊥ JOCHEN SCHMITT,†,‡,⊥ AND THOMAS F. STOCKER†,‡

Climate and Environmental Physics, Physics Institute, University of Bern, Bern, Switzerland, Oeschger Centre for Climate Change Research, University of Bern, Bern, Switzerland, British Antarctic Survey, Cambridge, United Kingdom, Centre for Ice and Climate, Niels Bohr Institute, University of Copenhagen, Denmark, and Alfred-Wegener-Institute for Polar and Marine Research, Bremerhaven, Germany

Received March 20, 2008. Revised manuscript received July 18, 2008. Accepted July 29, 2008.

Continuous flow analysis (CFA) is a well-established method to obtain information about impurity contents in ice cores as indicators of past changes in the climate system. A section of an ice core is continuously melted on a melter head supplying a sample water flow which is analyzed online. This provides high depth and time resolution of the ice core records and very efficient sample decontamination as only the inner part of the ice sample is analyzed. Here we present an improved CFA system which has been totally redesigned in view of a significantly enhanced overall efficiency and flexibility, signal quality, compactness, and ease of use. These are critical requirements especially for operations of CFA during field campaigns, e.g., in Antarctica or Greenland. Furthermore, a novel device to measure the total air content in the ice was developed. Subsequently, the air bubbles are now extracted continuously from the sample water flow for subsequent gas measurements.

Introduction

Ice cores provide a wealth of information about past climate (*1, 2*), reaching back as far as 800 kyr in time. The diversity of dissolved and particulate impurities deposited on ice sheets provides an opportunity to obtain information on changes in atmospheric transport and chemistry, strengths of sources and sinks, and depositional effects (*3*−*5*).

Over the past years, continuous flow analysis (CFA) systems have become a standard in ice core analyses (*6*−*11*). This is due to the very fast and efficient decontamination of the sample and the high depth resolution that can be achieved over the full length of a deep ice core, in a fraction of the time compared to that required for discrete sampling methods. In CFA, a longitudinal subsection of an ice core is melted continuously on a melter head, located in a cold environment, while the sample is separated into inner and outer sample flows providing efficient decontamination of the sample (*9, 10, 12, 13*). The inner sample section, which consists of the meltwater and bubbles from enclosed air in the ice, is continuously pumped into a warm laboratory for online analyses. Different analysis techniques can be used in a CFA system. Apart from the methods used in this work, mass spectrometers (*7*−*9*), fast ion chromatographs (FIC) (*6, 11*), or other techniques (*14*) can be connected to a CFA melting device.

The CFA system developed at the University of Bern, based on earlier work (*12, 13*) and several innovations described here, has been successfully used to obtain ice core records in the frame of the recent major European ice core projects in Antarctica (e.g., refs *3, 15*). However, the original CFA setup has been lost during ship transport from Antarctica. This gave us the chance to design a new system in a rigorous field deployable way and to include several innovations: novel measuring units have been introduced and existing ones have been improved.

Past fieldwork has shown the need for a compact, modular, robust, and transportable CFA system with temperature stabilization. In situ analysis of ice cores in the field is advantageous as the ice samples do not have to be transported and hence the risk of additional fractures is avoided. This is technically very important for the feasibility of the continuous melting procedure, and scientifically to get high-resolution records with fewer gaps. Furthermore, the risk of contamination (e.g., HCHO) is reduced.

In this publication we describe new measuring units for CFA such as the analysis of the total air content (TAC) and insoluble dust particle concentration and size distribution (*16*). The CFA system now also features a continuous air extraction unit, offering the possibility of subsequent gas analysis. Until now, the air in the melt flow originating from the ice has been released without scientific benefit, although these bubbles contain valuable information about the composition of the past atmosphere (*17, 18*). In addition, a novel technique for total organic carbon (TOC) has been developed. However, its description is beyond the scope of this publication and is provided in a separate publication (*26*). Furthermore, several improvements or innovations concerning traditional Bern CFA units (*12*) are described briefly. To demonstrate the capability of our improved CFA system we present measurements of TAC, dust, Na^+, Ca^{2+}, NH_4^+, NO_3^-, SO_4^{2-}, H_2O_2, HCHO, and the electrolytical conductivity on a sequence of the North Greenland Ice Core Project (NGRIP) ice core.

In addition to the innovations of the present work, the major goal was to completely redesign the whole system in order to improve the overall efficiency, signal stability, robustness, automation, and ease of use. Hence, discussion of the system is organized in preassembled units: melting unit, sample distribution unit, and analysis unit.

Melting Unit

From the ice core, a sample with a typical cross section of 32×32 mm^2 and a length between 1.0 and 1.65 m is cut and then vertically placed above a heated melter head in a PTFE-coated aluminum tray, which guides the ice during melting. The whole melting unit is rack-mounted and located in a cold environment at around −20 °C. It also contains a LCD display and control buttons to monitor and control the CFA system from the cold laboratory.

* Corresponding author e-mail: kaufmann@climate.unibe.ch; phone: +41 (0)31 631 4465; fax: +41 (0)31 631 8742.
† Climate and Environmental Physics, Physics Institute, University of Bern.
‡ Oeschger Centre for Climate Change Research, University of Bern.
§ British Antarctic Survey.
∥ University of Copenhagen.
⊥ Alfred-Wegener-Institute for Polar and Marine Research.

10.1021/es8007722 CCC: $40.75
Published on Web 10/04/2008

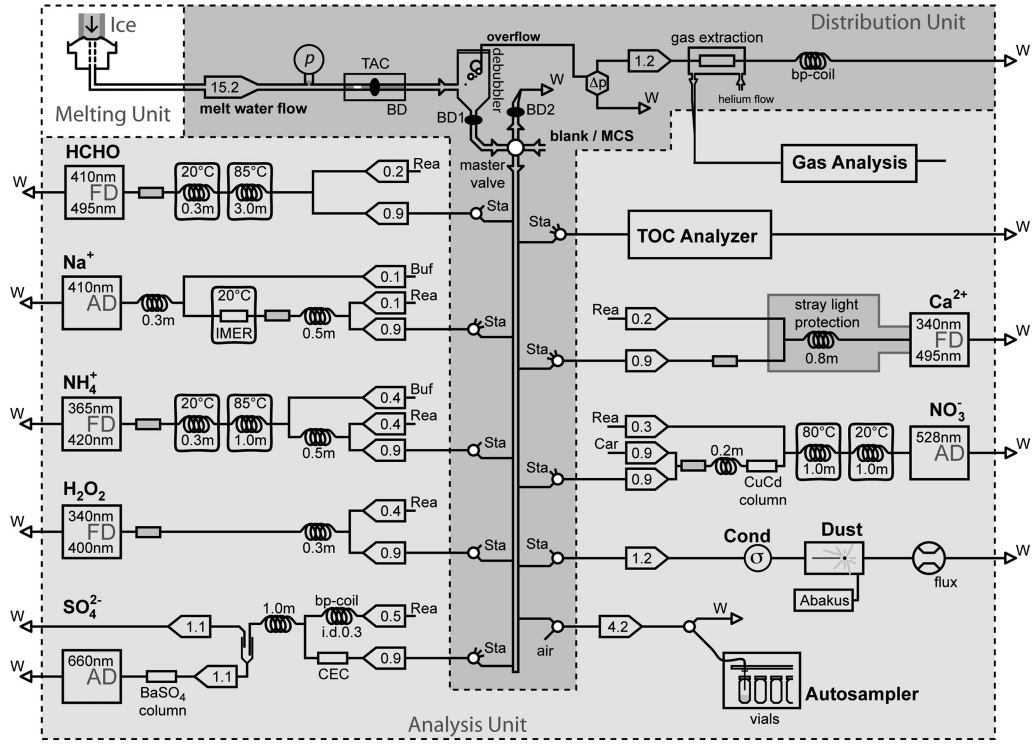

FIGURE 1. The flow system of the CFA analysis system. Meltwater flow from the melting unit is divided by the use of a closed debubbler into a bubble-free sample water flow and an air-containing overflow. The latter is led to a gas extraction unit for further gas analysis, while the sample water passes through the master valve and is distributed to the measuring units. Abbreviations and symbols: total air content (TAC), Solenoid valves (small white circles), bubble detectors (BD, black ellipses), pressure gauge (p), pump tubes and flow directions (arrow boxes), flow rates in mL/min (numbers in the arrow boxes), Accurel micro porous membrane debubbler (small gray boxes), fluorimetric detection (FD), absorption detection (AD), standard solution (Sta), reagent (Rea), carrier solution (Car), buffer solution (Buf), waste (W), immobilized enzyme reactor (IMER), cation exchange column (CEC), multicomponent calibration solution (MCS), buffer volume for pressure decoupling (Δp), and back pressure coil (bp-coil). Furthermore, lengths and temperatures (if heated or cooled) of mixing and reactor coils, and wavelengths of the different detections are indicated in the figure. Descriptions of additional items are given in the text.

Compared to earlier versions of the melter head (*12, 13*), the new design allows a larger sample rate and a more steady melting process. It has already proven its reliability by melting several 1000 m of ice cores. The melter head is now made of copper plated with electroless nickel (5 μm) and gold (2 μm) to provide a chemically inert surface with good thermal conductivity. The surface is divided into two concentric parts (Figure FS2 in the Supporting Information, SI), but only the sample water from the inner part (diameter of 24 mm) is used for analysis. To prevent contamination efficiently, a small meltwater overflow from the inner toward the outer part is guaranteed (*7, 8*). This is achieved by pumping less sample water from the inner part than available at the chosen melting speed.

Due to the enlargement six concentrically arranged drain-off holes are used, instead of one central hole. They are connected to a PEEK-manifold by connection tubes as short as possible, but of identical length, in order to minimize sample dispersion. From the manifold a PFA tube (1.55 mm i.d., 1/8″ o.d., Omnilab) leads to the warm laboratory. An additional six tubes from the outer part ensure drainage of the discarded meltwater which could be used for further investigations (e.g., for contamination insensitive isotope measurements (*19*)).

To maintain a constant melting rate of typically 3.5 cm/min, the melter head is kept at constant temperature (typically 20 °C). A thermostat (dTron16, JUMO) is connected to an electrical cartridge heater of 400 W (Electrolux) in the center of the copper body to provide heat coaxial to the ice sample. The melt progress is registered by an optical encoder (Baumer Electric) connected to a weight lying upon the ice sample, which applies additional pressure to maintain a uniform melting speed also toward the end of a measurement.

Distribution Unit

In the distribution unit, the sample meltwater from the melter head is conveyed by a peristaltic pump with Tygon tubing (both Ismatec) at a rate of typically ∼15.2 mL/min (Figure 1), adjusted to the melting speed. It is naturally segmented by air bubbles coming from enclosed air in the ice which account for approximately 10% of the volume. A custom-built bubble detector is scanning the segmented flow in the PFA tubing before it enters the debubbler, providing information about TAC (see Analysis section). The debubbler is hermetically sealed to ambient air, and its volume (∼300 μL) is optimized to reduce sample dispersion but still prevent any air bubbles entering the analysis systems. The rate of the overflow is given by the difference of the inflow and the water consumption of all measuring units.

The final separation of air and water in the overflow takes place in the degassing unit through a gas-permeable hydrophobic membrane (Accurel, Microdyn) where a helium flow outside the Accurel is used as carrier gas (*7*). It is important to pressure-decouple the degassing unit from the entire liquid chemistry flow system, as it affects the flow rates. This is achieved with an additional buffer volume, which is open to atmospheric pressure (Δp in Figure 1). The bubble detector, the debubbler, the buffer volume and the degassing unit are mounted inside a temperature stabilized box (25 ± 0.02 °C).

After the debubbler, a master valve (080T-Series, BioChem Valve) determines whether sample water or blank flows

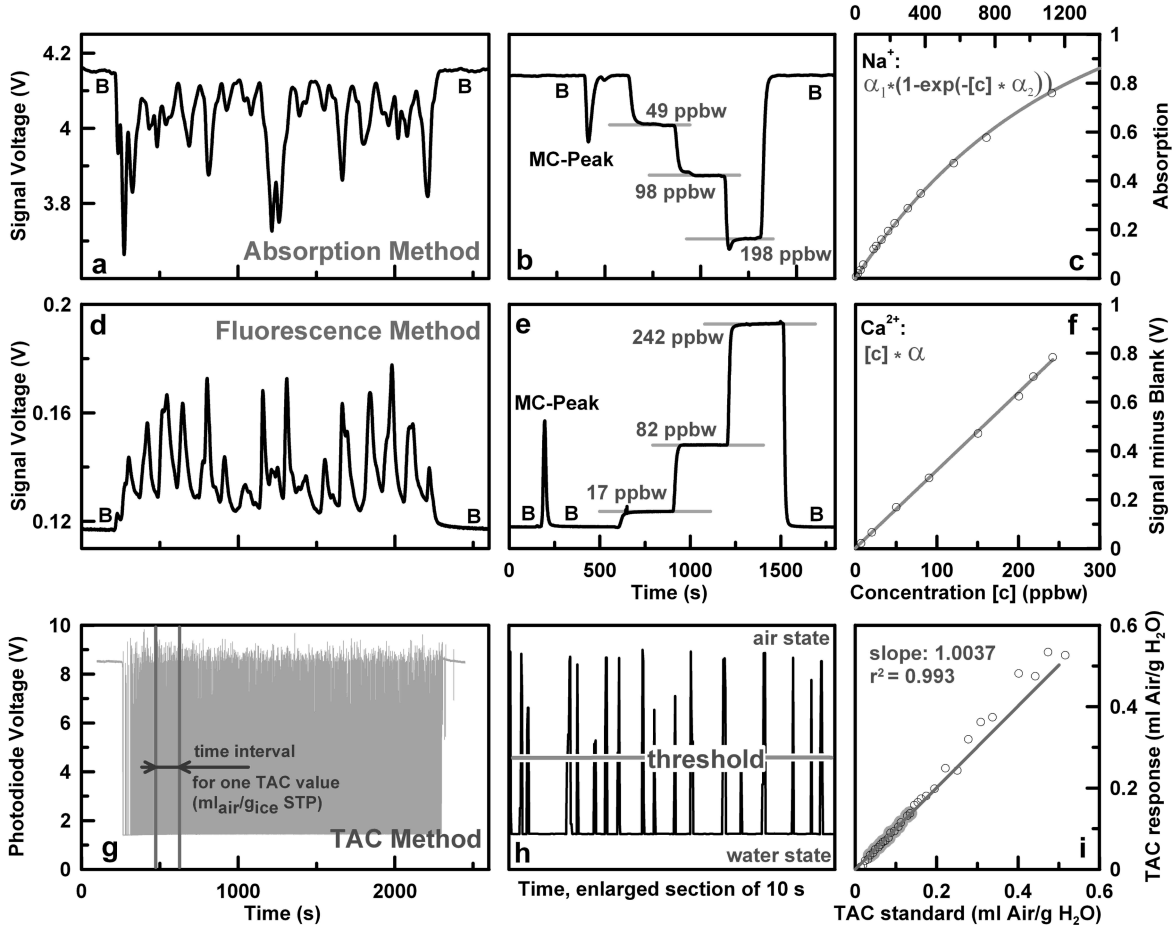

FIGURE 2. Typical measurement of a sample (110 cm) (a, d, g) and a calibration series (b, e). Na^+ is determined by an absorbance method, Ca^{2+} is measured using a fluorimetric method. The calibration series measurement (b, e) comprises also blank (B) and multicomponent standard solution (MC) signals. (c, f, i) show typical calibration curves and coefficients (based on larger calibration solution series than routinely done). The TAC measurement is calibrated by determining an effective threshold value dividing the signal into air or water state using an artificially segmented water flow of varying TAC (g, h). For the calibration only the TAC values in the range of 0.04−0.14 mL_{air} g_{ice}^{-1} are used.

toward the measuring units. As blank, Milli-Q water (Millipore Gradient A10, ≥18.2 MΩ/cm) is used, except for the HCHO detection where still mineral water (Evian) defines the blank level (*13*). Bubble detectors before and after the master valve (described in the TAC section), automatically detect the start and the end of the sample flow and switch the master valve accordingly to prevent air entering the detection units. Instead of blank, a multicomponent calibration solution can be introduced to the system. This new feature allows the determination of the individual time delays between the master valve and the different detectors. They are key parameters for the automated data processing software in order to align the records on the common depth scale of the ice core.

Subsequently, the sample flow is split into different lines for each measuring unit. Each line is equipped with a solenoid valve to alternately feed specific calibration solutions. This is done every 2 h, i.e., after 4 m of measured ice. With a custom-made electronic control unit, each valve can either be switched manually or software controlled. The whole sample unit is controlled by interface devices (CompactRIO Modules NI9401, 9477, National Instruments NI) and software written in Labview (Version 8.21, NI) running on the CompactRIO.

Analysis Unit

Optical Method for the Measurement of Total Air Content (TAC). In contrast to other methods for the measurement of TAC which are based on discrete sampling (*20*), a new technique for TAC analysis was developed which determines the content of air by continuously scanning the sample flow from the melter head with a custom-built bubble detector (Figure 1). Absolute TAC values (mL_{air} g_{ice}^{-1}, STP) are calculated for every interval of 3 min (see Discussion) from the ratio between the times the bubble detector records air or water. These calibrated values are then corrected for temperature, pressure, and solubility effects.

The bubble detector is a light barrier made of a LED aligned with a photo transistor scanning through the transparent PFA tubing (1.55 mm i.d., 1/8″ o.d., Omnilab). The whole TAC device is mounted in a temperature-stabilized box at 25 ± 0.02 °C. The pressure within the sample flow is measured by a pressure gauge (LEO3, 0−4 bar, Keller) which is connected by a custom-made T-fitting. In this fitting the dead volume of the pressure gauge is separated from the sample flow with a movable Teflon pin which transmits the pressure changes. This component is required to minimize signal dispersion for the continuous chemical measurements.

The analog signal of the photo transistor voltage is recorded every 50 ms and a threshold divides this signal in a water and air state (Figure 2h). For its setting and, thus, the calibration of the bubble detector, an artificially segmented flow is generated by an air and a water flow controller (F-200CV and L23V02, Bronkhorst) connected to a T-fitting. The flow controllers are fed with technical air (in the following assumed to contain 79% N_2 and 21% O_2) and Milli-Q water previously degassed by bubbling with helium. Helium is also used to apply the necessary primary pressure on the Milli-Q

water to feed the water flow controller. Due to different solubilites and hence partial pressures of N_2, O_2, and He in water and gas phase, the segmented flow reaches a new equilibrium, which also affects the volume of gas bubbles. The time to reach equilibrium is ~5 s, which was determined by varying the tube length before the bubble detector and thus the interaction time during calibration. This is considerably faster than the time between melting and TAC detection (~35 s).

To correct for the different gas solubilities in water, a 2-box model for 3 gases was set up. One box with fixed volume contains all the water while the second box contains the gas phase. Initially for the calibration, helium is only dissolved in the water while the air is only in the gas phase. In equilibrium, all gases are present in both phases which changes also the volume of the gas bubbles V_{air}. This change can be calculated by solving eqs 1 and 2, where p_i are the partial pressures, p is the total pressure, n_i is the gas quantities, k_i is the solubilities, V_{H_2O} is the water volume, R is the gas constant, and T is the stabilized temperature in the box.

$$p = \sum p_i \qquad (i = N_2, O_2, He) \tag{1}$$

$$n_i = p_i V_{air}/(RT) + k_i p_i V_{H2O} \tag{2}$$

To derive calibrated and solubility corrected TAC values we used a two step approach. For a calibration, V_{air} is calculated while the n_i are known from the flow controllers and the primary pressure of the helium. A threshold in the light detector signal is defined (Figure 2h) above which the signal is interpreted as air and below which is interpreted as water flow. The level of the threshold is then adjusted so that the resulting air/water ratio corresponds to the ratio of the artificial, controlled segmented flow (in equilibrium).

For the measurements, the TAC values are calculated by evaluating the bubble detector signal at the given threshold over time intervals of 3 min (Figure 2g). Subsequently these values are corrected for the solubilities of N_2 and O_2 using eqs 1 and 2 to obtain the total volume of air ($mL_{air}\ g_{ice}^{-1}$, STP) present in the ice core sample.

Continuous Measurements on the Sample Water Flow. All the measuring units are mounted in individually temperature-stabilized (±0.05 °C) modules ($70 \times 240 \times 150\ mm^3$) to hold the measurement at its specific temperature (see Discussion). Moreover, this new feature minimizes baseline drifts and signal noise induced by temperature changes. The dynamic range of the temperature stabilization of approximately 20 °C is broad enough to achieve optimal sensitivities for the individual detections and to compensate for laboratory temperature fluctuations which are common under field conditions.

The detection methods were adopted from refs *12, 13, and 21*, but individually upgraded. For the sodium method, the pH is now increased by continuously adding a 17 mM ammonia solution to the flow after the reaction column (IMER). The sulfate method was completely redesigned (*21*) using an absorbance method which is simpler in operation. The detection limit of 70 ppbw (given in ref *21*) was further reduced to 10 ppbw by adjusting the backpressure regime for the input tubes. This was achieved by introducing additional tube pieces (0.3 mm i.d.) of appropriate lengths. For the NH_4^+, NO_3^-, and HCHO detection, the mixed flow is additionally heated to accelerate the chemical reaction and therefore to increase the detection sensitivity. Subsequently, active cooling to ambient temperature reproducibly decelerates the reactions and dissolves emerging micro bubbles. The novel self-made heating and cooling reactors consist of PFA tubing molded in low-temperature melting alloy (BiSn, melt temperature 138 °C) and are either heated by heater foil (Minco) or cooled by thermoelectric coolers (Melcor) which both are controlled by thermostats (JUMO). Applied temperatures and tubing lengths are indicated in Figure 1.

Completely new detectors, both for fluorescence and absorbance methods (Figure 1), were constructed in a compact design ($45 \times 140 \times 80\ mm^3$). The previously used very delicate phosphor-coated mercury lamps were replaced with light-emitting diodes (LEDs, Roithner Lasertechnik) which provide a selective excitation wavelength, high spectral intensity, and low power consumption. For fluorimetric detection, the photosensor modules are mounted orthogonal to the LED light source. In the light path, a mirrored micro flow cell (18 μL, custom product by Hellma) is used (*12*). For the absorbance detection, a flow-through cell (178.010-QS, Hellma) leads the absorbing sample solution into the light path with a length which is appropriate for the expected concentrations (10−40 mm). For light detection, small photosensor modules (H9306-02, Hamamatsu) are used, in combination with specific optical band-pass filters (LOT Oriel, bandwidth 10 nm). The individual filter and LED peak wavelengths for each detection method are given in Figure 1. To suppress electronic and magnetic interferences, the photosensor modules are encased in a custom-made electromagnetic shielding (high magnetic permeability alloy, Meca Magnetics).

Besides the chemical measurements, a particle detector with a control device (Abakus with sensor type LDS-12/25, Klotz) was adapted for measuring insoluble particles and their size distribution (*16*). The sample water passes through a flow cell where the particle sizes are determined by a laser beam with a wavelength of 670 nm. The particle size is recorded in 32 bins in a particle diameter range of typically 1.0 to 15 μm. Size calibration is performed in a complex procedure using comparative measurements of identical samples with a Coulter Counter (Beckman) (*16*). The flow rate is now measured by a flow-through sensor (ASL1430, Sensirion), to convert the number of particles per second to number per mL. To test for potential size fractionation effects in the distribution unit, we measured particle size distributions dependent on different flow line configurations and pump speeds. This showed no systematic size fractionation effects within the detection limits. A recent intercomparison of different methods for analysis of mineral dust in ice cores describes the performance of this system (*22*). Measurement of the electrolytic conductivity is achieved by a micro flow cell (cell constant of 100 cm^{-1}, volume of 120 μL) connected to a conductivity meter (AS1056, both Amber Science).

An autosampler (*23*), collecting uncontaminated sample water in vials for subsequent discrete analyses (e.g., ref *5*), is also connected to the distribution unit. For all flow lines, PFA tubing (0.5 mm i.d., 1/16″ o.d., Omnilab) is used. Pumping is achieved by Tygon pump tubes in a peristaltic pump (Ismatec), except for the sulfate method, where Pharmed/Ismaprene pump tubes are used because of the ethanol-containing reagent (*21*). In most of the measuring units a short piece of Accurel membrane tubing is inserted before the detectors to remove remaining micro bubbles that would disturb the signal. All detector voltage signals are acquired as one-second averages with CompactRIO modules NI9205 (NI) and the same custom-made Labview software which also controls the distribution unit.

Data Processing

Measurement of various species with one data point every second leads to a large amount of raw data from km-long ice cores. The raw data have to be processed and manually quality checked. To streamline this time-consuming task and to make preliminary processed data available right after the measurements, new data-processing software based on MATLAB (Mathworks) was developed. The program calculates the

concentrations (in ppbw) from the raw signal (in V) in two steps. First, in every calibration file the program automatically determines the voltage levels of the known standard solutions and of the blank water signal. For this a pattern-comparison algorithm with a step function is used. Then the trend of the baseline, defined by the linear interpolation between the two blank levels is removed from the calibration signal. Linear (Ca^{2+}, NH_4^+, NO_3^-, SO_4^{2-}, HCHO, H_2O_2) or exponential curve fits (Na^+, Figure 2c) yield the calibration factors (V ppbw^{-1}) for each species. In the second step, the resulting calibration factors are used to compute the concentrations from the raw ice core data, again after automatically removing the baseline. Finally, the concentrations are transferred to the common depth scale of the ice core using the encoder data and considering the individual time delays of each component. For this, the program makes use of system status information that was recorded during measurements, e.g., the time delay between the automatic injection of a multicomponent solution pulse by the master valve and the registration of the corresponding peak in the individual detectors (Figure 2b,e). These time delays vary, e.g., as pump tubings age. The resulting preliminary data sets are available immediately after processing. However, for the final data set a thorough quality control of all automatically processed data has to be done. For example, data of potentially contaminated ice (e.g., at breaks) and spikes from air bubbles and electronic artifacts still have to be removed manually.

Results and Discussion

With our improved CFA system, a section from the North Greenland Ice Core Project (NGRIP (*24*)) was measured. It comprises stratigraphic layers of an age of about 10.15 kyr BP (Figure FS3 in the Supporting Information). Clear annual cycles can be observed in most of the species. The reproducibility of the CFA has been tested by analyzing two parallel ice stripes of 0.55 m each (Figure 3). The measurement of the second stripe was performed in reverse direction to visualize potential effects of the nonsymmetric dispersion of the sample in the system. The measurements show a very good agreement reproducing the cm-scale variations present in ice core records; the seasonal chronology with high concentrations of NH_4^+ in summer, Ca^{2+} and dust peaks in spring, and high Na^+ in winter is apparent.

The results of the TAC measurement (Figure FS3 in the Supporting Information) show variations that could not be resolved by previous discrete TAC analysis methods. To confirm the obtained values, comparison measurements were carried out with a barometric method, coupled to a gas extraction by sublimation of ice samples. The measurements are in good agreement within the respective error limits supporting quantitative TAC measurements using our CFA method (see Supporting Information for a description of the method and the results).

The new TAC technique features an accuracy of 0.4%, and the calibration shows an excellent linearity ($R^2 = 0.993$) over the whole measurement range from 0.04 to 0.14 $mL_{air}\ g_{ice}^{-1}$ (Figure 2i), which covers previous TAC measurements from various locations in Greenland and Antarctica (*25*). To determine the optimal evaluation interval for the TAC analysis (highest temporal resolution and low statistical noise), different intervals (from 10 s to 6 min) were tested by comparing the standard deviation of 10 consecutive calibration measurements. For evaluation intervals larger than 3 min, the standard deviation is constant at 2% but increases significantly below 3 min. Accordingly we state a precision of 2% of our TAC measurement for 3 min evaluation intervals. For a typical melting speed of 3.5 cm/min, this leads to a depth resolution of the TAC analysis of ~10 cm at maximum sensitivity.

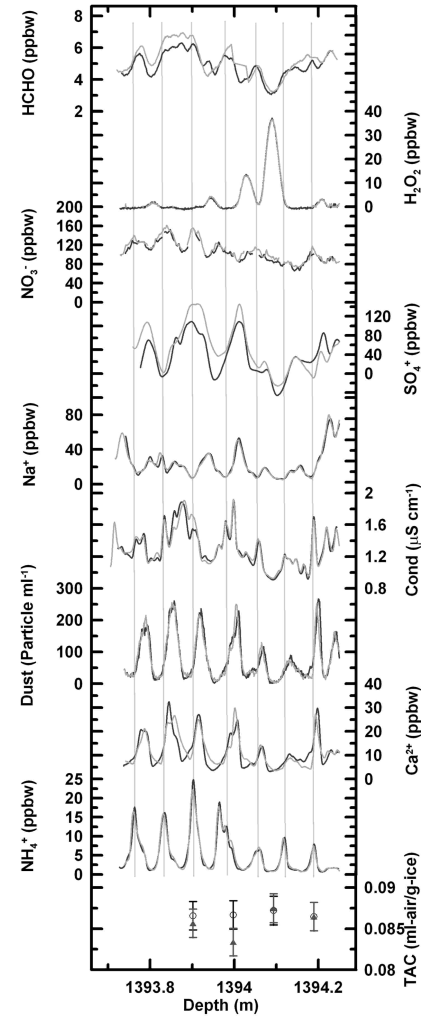

FIGURE 3. Results of the reproducibility measurement on NGRIP ice. The gray line (TAC, dots) represents the first measurement, while the black line (TAC, triangle) shows the second, measured in the opposite direction. The vertical light gray lines mark the NH_4^+ summer peaks to emphasize the seasonal phasing. All data are plotted at 1 mm resolution except HCHO, which has been smoothed with a 13 mm running mean to reduce electronic noise. For TAC, a data point every 10 cm is shown with an error bar of 2%.

For the other measuring units, the limit of detection is calculated as 3 times the standard deviation of blank measurements. It is 10 ppbw for SO_4^{2-}, and in the range of 0.1−1 ppbw for other species as published earlier (*12, 13*). The temporal resolution defined as the time required for the signal of a step function (switch from blank to calibration solution) to rise from 10% to 90% of the final height is around 14 s for conductivity, H_2O_2, dust, and Ca^{2+}, 20 s for NH_4^+, 32 s for Na^+, HCHO, and NO_3^-, and 45 s for SO_4^{2-}. Considering a melting speed of 3.5 cm/min, this leads to a depth resolution in the ice of approximately 0.8, 1.2, 1.9, 2.6, and 3.5 cm, respectively. The SO_4^{-2} data in Figure 3 were corrected for pressure changes during the measurements due to failing pump tubing. This failure is also the reason for some negative SO_4^{2-} values in Figure 3.

Fluctuations in the warm laboratory temperature have often been the limiting factor for signal stability, especially during field measurements. The temperature sensitivities of the individual detection methods of CFA were systematically determined for the first time by measuring calibration solutions at various temperatures with the new temperature-controlled measuring units (Figure 4). We found specific

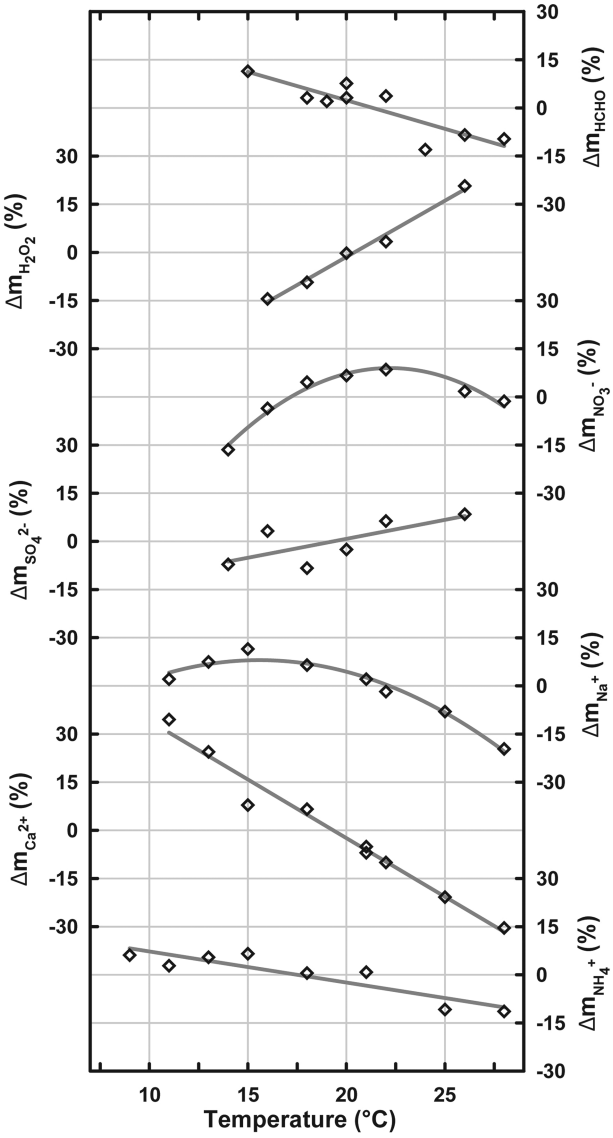

FIGURE 4. Temperature sensitivities of the individual detection methods. The relative gradient (m) refers to the slope of the calibration curve (V ppbw^{-1}) or in case of sodium, to the slope of the tangent to the calibration curve at zero, divided by the mean gradient.

optimum operation temperatures for the Na^+ method at 16 °C and for NO_3^- at 22 °C. The H_2O_2 measurement is more sensitive at higher temperatures, whereas the sensitivity of the Ca^{2+} method increases with lower temperatures. The responses of the NH_4^+, HCHO, and SO_4^{2-} methods to temperature are weak. These results show that temperature stabilization is essential for most species.

The improved CFA system now features a modular and expandable design. It was significantly reduced in size and weight and built more robustly. At the same time the number of measurable parameters has been increased. Each of the three rack-based units can now be transported fully preassembled and optimized in a 0.25 m^3 box (Zarges, picture PS5 in the Supporting Information). This decreases the setup and testing time in the field substantially. But transportability also means that we are able to easily ship the CFA system to another host institute for collaborative work. Signal stability was greatly improved with the new temperature-controlled modules, which is crucial especially for field deployments where stable laboratory temperatures are generally not achievable. The much higher degree of automation of the improved CFA system and the data processing considerably increased its overall efficiency and user friendliness so that one person can operate the CFA system if necessary. A typical measuring performance of 30 m of ice per 24 h including the preprocessing of the data is achieved at the normal melt speed of 3.5 cm/min.

Acknowledgments

Financial support by the Swiss National Science Foundation is acknowledged. We thank Remo Walther, Hans-Peter Moret, and Peter Nyfeler for technical support and input, Jørgen Peder Steffensen and the NGRIP team for the ice samples, Dietmar Wagenbach (University of Heidelberg) for the development of the autosampler, Hubertus Fischer and the reviewers for their fruitful comments. This document was produced with the financial help of the Prince Albert II of Monaco Foundation.

Supporting Information Available

A brief description of the barometric TAC analysis and the results; results of the test measurement of NGRIP ice samples and several images of the new CFA setup. This information is available free of charge via the Internet at http://pubs.acs.org

Literature Cited

(1) EPICA community members. Eight glacial cycles from an Antarctic ice core. *Nature* **2004**, *429* (6992), 623–628.
(2) EPICA community members. One-to-one coupling of glacial climate variability in Greenland and Antarctica. *Nature* **2006**, *444* (7116), 195–198.
(3) Fischer, H.; Siggaard-Andersen, M. L.; Ruth, U.; Röthlisberger, R.; Wolff, E. Glacial/interglacial changes in mineral dust and sea-salt records in polar ice cores: Sources, transport, and deposition. *Rev. Geophys.* **2007**, *45*, doi:10.1029/2005RG000192.
(4) Legrand, M.; Mayewski, P. Glaciochemistry of polar ice cores: A review. *Rev. Geophys.* **1997**, *35* (3), 219–243.
(5) Wolff, E. W.; Fischer, H.; Fundel, F.; Ruth, U.; Twarloh, B.; Littot, G. C.; Mulvaney, R.; Röthlisberger, R.; de Angelis, M.; Boutron, C. F.; Hansson, M.; Jonsell, U.; Hutterli, M. A.; Lambert, F.; Kaufmann, P.; Stauffer, B.; Stocker, T. F.; Steffensen, J. P.; Bigler, M.; Siggaard-Andersen, M. L.; Udisti, R.; Becagli, S.; Castellano, E.; Severi, M.; Wagenbach, D.; Barbante, C.; Gabrielli, P.; Gaspari, V. Southern Ocean sea-ice extent, productivity and iron flux over the past eight glacial cycles. *Nature* **2006**, *440* (7083), 491–496.
(6) Cole-Dai, J. H.; Budner, D. M.; Ferris, D. G. High speed, high resolution, and continuous chemical analysis of ice cores using a melter and ion chromatography. *Environ. Sci. Technol.* **2006**, *40* (21), 6764–6769.
(7) Huber, C.; Leuenberger, M.; Zumbrunnen, O. Continuous extraction of trapped air from bubble ice or water for on-line determination of isotope ratios. *Anal. Chem.* **2003**, *75* (10), 2324–2332.
(8) Knüsel, S.; Piguet, D. E.; Schwikowski, M.; Gäggeler, H. W. Accuracy of continuous ice-core trace-element analysis by inductively coupled plasma sector field mass spectrometry. *Environ. Sci. Technol.* **2003**, *37* (10), 2267–2273.
(9) McConnell, J. R. Continuous ice-core chemical analyses using inductively coupled plasma mass spectrometry. *Environ. Sci. Technol.* **2002**, *36* (1), 7–11.
(10) Osterberg, E. C.; Handley, M. J.; Sneed, S. B.; Mayewski, P. A.; Kreutz, K. J. Continuous ice core melter system with discrete sampling for major ion, trace element, and stable isotope analyses. *Environ. Sci. Technol.* **2006**, *40* (10), 3355–3361.
(11) Traversi, R.; Becagli, S.; Castellano, E.; Migliori, A.; Severi, M.; Udisti, R. High-resolution fast ion chromatography (FIC) measurements of chloride, nitrate and sulphate along the EPICA Dome C ice core. *Ann. Glaciol.* **2002**, *35*, 291–298.
(12) Röthlisberger, R.; Bigler, M.; Hutterli, M.; Sommer, S.; Stauffer, B.; Junghans, H. G.; Wagenbach, D. Technique for continuous high-resolution analysis of trace substances in firn and ice cores. *Environ. Sci. Technol.* **2000**, *34* (2), 338–342.
(13) Sigg, A.; Fuhrer, K.; Anklin, M.; Staffelbach, T.; Zurmühle, D. A continuous analysis technique for trace species in ice cores. *Environ. Sci. Technol.* **1994**, *28* (2), 204–209.

(14) McConnell, J. R.; Edwards, R.; Kok, G. L.; Flanner, M. G.; Zender, C. S.; Saltzman, E. S.; Banta, J. R.; Pasteris, D. R.; Carter, M. M.; Kahl, J. D. W. 20th-century industrial black carbon emissions altered arctic climate forcing. *Science* **2007**, *317* (5843), 1381–1384.
(15) Bigler, M.; Rothlisberger, R.; Lambert, F.; Stocker, T. F.; Wagenbach, D. Aerosol deposited in east Antarctica over the last glacial cycle: Detailed apportionment of continental and sea-salt contributions. *J. Geophys. Res.-Atmos.* **2006**, *111*, D8.
(16) Ruth, U.; Wagenbach, D.; Bigler, M.; Steffensen, P.; Röthlisberger, R.; Millar, H. High-resolution microparticle profiles at North-GRIP, Greenland: Case studies of the calcium-dust relationship. *Ann. Glaciol.* **2002**, *35*, 237–242.
(17) Raynaud, D.; Lipenkov, V.; Lemieux-Dudon, B.; Duval, P.; Loutre, M. F.; Lhomme, N. The local insolation signature of air content in Antarctic ice. A new step toward an absolute dating of ice records. *Earth Planet Sci Lett* **2007**, *261* (3−4), 337–349.
(18) Spahni, R.; Chappellaz, J.; Stocker, T. F.; Loulergue, L.; Hausammann, G.; Kawamura, K.; Fluckiger, J.; Schwander, J.; Raynaud, D.; Masson-Delmotte, V.; Jouzel, J. Atmospheric methane and nitrous oxide of the late Pleistocene from Antarctic ice cores. *Science* **2005**, *310* (5752), 1317–1321.
(19) Winckler, G.; Fischer, H. 30,000 years of cosmic dust in Antarctic ice. *Science* **2006**, *313* (5786), 491–491.
(20) Lipenkov, V.; Candaudap, F.; Ravoire, J.; Dulac, E.; Raynaud, D. A new device for the measurement of air content in polar ice. *J. Glaciol.* **1995**, *41* (138), 423–429.
(21) Bigler, M.; Svensson, A.; Steffensen, J. P.; Kaufmann, P. A new continuous high-resolution detection system for sulphate. *Environ. Sci. Technol.* **2007**, *45*, 178–182.
(22) Ruth, U.; Barbante, C.; Bigler, M.; Delmonte, B.; Fischer, H.; Gabrielli, P.; Gaspari, V.; Kaufmann, P.; Lambert, F.; Maggi, V.; Marino, F.; Petit, J.-R.; Udisti, R.; Wagenbach, D.; Wegner, A.; Wolff, E. W. Proxies and measurement techniques for mineral dust in Antarctic ice cores. *Environ. Sci. Technol.* **2008**, *42* (15), 5675–5681.
(23) Ruth, U.; Wagenbach, D.; Mulvaney, R.; Oerter, H.; Graf, W.; Pulz, H.; Littot, G. Comprehensive 1000 year climatic history from an intermediate-depth ice core from the south dome of Berkner Island Antarctica: methods dating and first results. *Ann. Glaciol.* **2004**, *39*, 146–154.
(24) North GRIP members. High-resolution record of Northern Hemisphere climate extending into the last interglacial period. *Nature* **2004**, *431* (7005), 147–151.
(25) Martinerie, P.; Raynaud, D.; Etheridge, D. M.; Barnola, J. M.; Mazaudier, D. Physical and climatic parameters which influence the air content in polar ice. *Earth Planet Sci Lett* **1992**, *112* (1−4), 1–13.
(26) Federer, V.; Kaufmann, P. R.; Manuel, H. A.; Simon, S.; Stocker, T. Continuous Flow Analysis of total organic carbon in polar ice cores. *Environ. Sci. Technol.* **2008**, *42*, 8039–8043.

ES8007722